Supporting Information

Theoretical study of the source-drain current and gate leakage current to understand the graphene field-effect transistors

Cui Yu, [1] Hongmei Liu, [1] Wenbin Ni,[1] Nengyue Gao,[1]Jianwei Zhao,[1*] Haoli Zhang[2]

[1]Key Laboratory of Analytical Chemistry for Life Science (Ministry of Education), School of Chemistry and Chemical Engineering, Nanjing University, Nanjing 210008, P. R. China
[2]State Key Laboratory of Applied Organic Chemistry and College of Chemistry and Chemical Engineering, Lanzhou University, Lanzhou, Gansu 730000, P. R. China

**Author to whom correspondence should be addressed: zhaojw@nju.edu.cn*

Contents:

1. Electron transport in the SA-*N* series

Fig. S1a plots the HOMO, LUMO and HLG energy levels of the SA-*N* series at zero bias, in which the Fermi level of the gold electrode is set to be *zero*. HOMO increases a little firstly, and then decreases from SA-1 to SA-5. On the contrary, LUMO increases monotonously. The HLG values vary insignificantly between 0.86 and 0.98 eV, indicating that the side substitution does not modify the main electronic structure of the conjugation system.

Another static feature of the molecular junction is the spatial distribution, which partially represents the mobility of the π-electron in the molecular system.[1-3] Fig. S1b displays the distribution of the frontier molecular orbitals for the SA-*N* series. For the shortest channel SA-1, the molecular orbitals locate on the top side of the molecule along the electron transport route, regardless of the bias is applied. When the substitution is changed, the spatial distribution displays different patterns. For the cross channels *N*=2-5, the distribution of HOMO and LUMO spreads to the body of molecular wire. This observation indicates that the main body of electron transport in the models *N*=2-5 may be similar in various terminal substitution positions.

All these static features infer some similarity in the electron transport behavior among the above samples. Fig. S1c gives the current as a function of the junction bias for the first series of models. In general, the current has a rapid increase in the low bias from -0.2 V to 0.2 V, and varies slowly at high bias, showing an “S” shape I-V curve. The shortest channel has the largest current at any time since the shortest transport route is applied. But for other cross channels *N*=2-5, the I-V curves are also close to that of the shortest channel. This obsevation means that all cross channels have similar electron transport behavior with high efficiency as compared with the

shortest channel, though some of them are along the perpendicular direction to the electric field.

(a) (b)

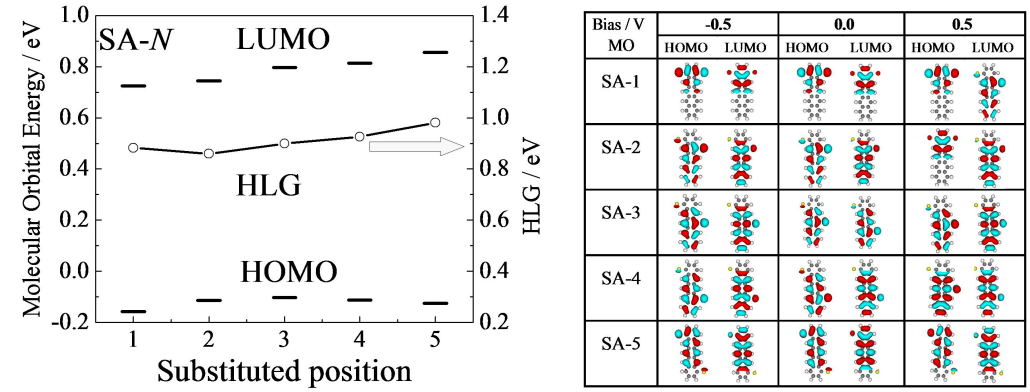

(c) (d)

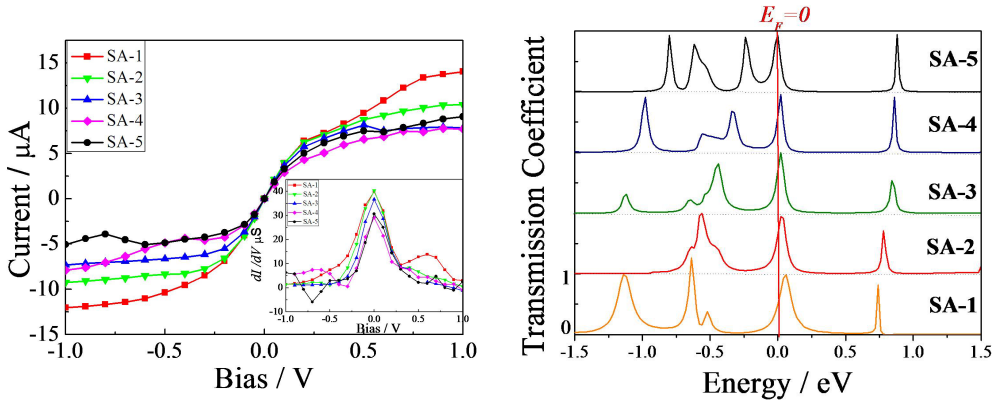

Fig. S1 (a) HOMO, LUMO, and HLG energy levels at zero bias, (b) The spatial distribution of the molecular orbitals close to the Fermi energy level, (c) The current-voltage curves, (d) Transmission spectra $T(E)$ as a function of electron energy at zero bias of the SA-*N* series;

According to the Landauer formula[4-6], current is calculated by using the integration of the transmission coefficient in the bias window. To explore the origin of the substitution, we further analyze the transmission spectra. Fig. S1d plots the transmission spectra as a function of the electronic energy at zero bias. The most notable feature is the sharp transmission wave with large transmission probability

closer to the Fermi energy. This peak can be mainly attibuted by the HOMO resonance as indicated by the HOMO level in the Fig. S1a. And the first transmission peak above the Fermi level is contributed by the LUMO resonance. Since the HOMO energy level is closer to the Fermi level, the zero-bias conductance is mostly caused by the HOMO resonance wave. All the cross channels have the similar feature to the shortest channel. From the similarity of the transmission spectrua, we may expect that the cross channels should have the similar transport behavior with the shortest channel. As discussed above, electron transport of the cross channels is as efficient as the shortest channel. Therefore, the current of multiple channels increases gradually with the increase of the graphene nanoribbons widths, as observed in the earlier experiment.[7, 8] It is possible to attach multiple leads to large molecule using the fabrication techniques.

2. The transmission spectra for the model molecules at different bias

The current has a rapid increase in the low bias, and varies slowly at high bias, showing an "S" shape I-V curve. It has been reported that the shape of the I-V curve was dependent on the particular molecule-electrode interface. When a hollow gold position is applied, the I-V curve may show a reverse "S" shape of I-V curve.[9] To explain it clearly, we plot transmission spectra of DA-*N*=1, 3, 5 at different bias, as shown in Fig. S1 a-c. It can be seen that the HOMO energy level is closer to the Fermi level. When a bias (V) is applied on the molecular junction, it essentially opens a bias window from E_F-eV/2 to E_F+eV/2 for the conduction electron (E_F is Fermi level of the junction). When the bias window is in the ranges from -0.5 V to +0.5 V, the integration of the transmission coefficient in the bias window increases as the bias

increases. However, at the high bias, though the bias window increases, due to lack of resonance peaks, the integration of the transmission coefficient in the bias window just slightly increases.

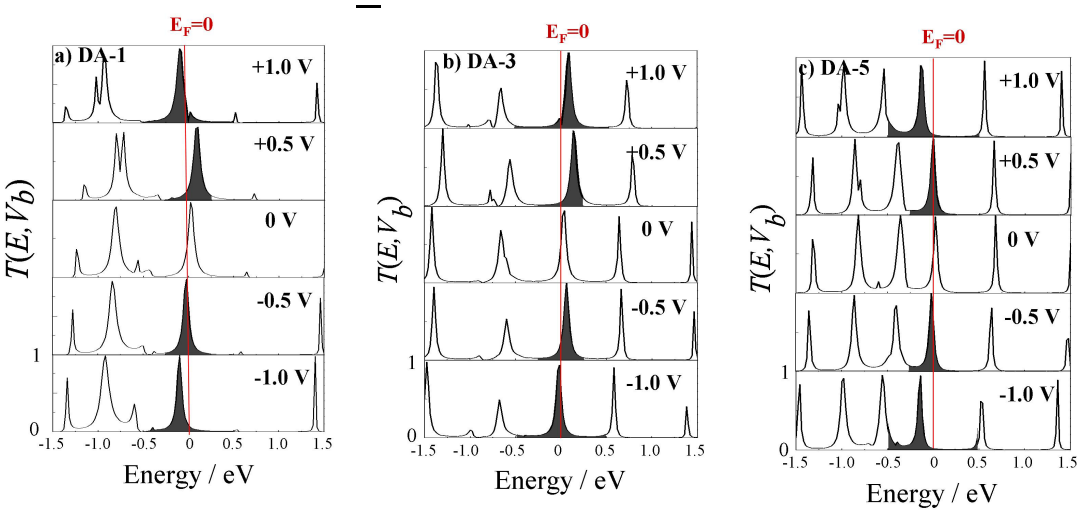

Fig. S2. The transmission spectra for the (a) DA-1, (b) DA-3, and (c) DA-5. The shadow region denotes the bias window.

3. Electron transport in defect acene molecular wires

In order to make further sight to the electron transport of cross channels, we design the models with defect, D-*N* (*N*=1, 5) and DD- *N* (*N*=1, 5), as shown in Fig. S3a.

For three models that *N*=1, the electron transport is along the shortest channel with similar electron transport route, but it has different current at any bias as shown in Fig. 3Sb. For the models that *N*=5, a clear order of the current can be observed for the models as DD-5 > TA-5 > D-5. Since the alternate double-single bond unit is the most probable electron transport pathway[10], both of the DD-5 and TA-5 have two possible pathway (red and green ways in Fig. 3Sa), but just one possible pathway for D-5, which might be the probable reason. We also calculate the current Ratio (Model-5/Model-1) given in the insert of the Fig. S3b to explore the electron transport of the cross channel. The perfect conductivity in the cross channel of the DD-5 is

observed. The Ratio order is DD-5 > TA-5 > D-5. The results demonstrate that the electron transport of the cross channels is efficient in the high conjugated acece molecular junction.

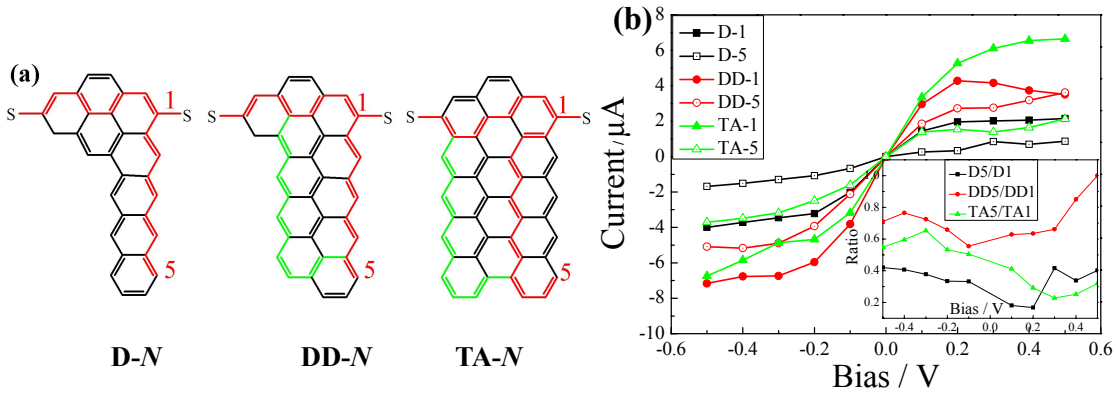

Fig. S3. (a) The models, and (b) the I-V curves of the defect acene molecular wires.

Reference:

1 X. Yin, H. M. Liu and J. W. Zhao, *J. Chem. Phys.*, 2006, **125**, 094711.

2 H. M. Liu, N. Wang, J. W. Zhao, Y. Guo, X. Yin, F. Y. C. Boey and H. Zhang, *Chem .Phys. Chem.*, 2008, **9**, 1416-1424.

3 J. M. Seminario, A. G. Zacarias and P. A. Derosa, *J. Phys. Chem. A*, 2001, **105**, 791-795.

4 *S. Datta : Electronic Transport in the Mesoscopic Systems (Cambridge University Press 1996).*

5 Y. Meir and N. S. Wingreen, *Phys. Rev. Lett* , 1992, 2512-2515.

6 R. Landauer, *IBM J. Res. Dev.*, 1957, **1**, 223-231.

7 M. Y. Han, B. Ozyilmaz, Y. B. Zhang and P. Kim, *Phys. Rev. Lett.* , 2007, **98**, 206805.

8 X. L. Li, X. R. Wang, L. Zhang, S. W. Lee and H. J. Dai, *Science*, 2008, **319**, 1229-1232.

9 M. Q. Long, L. L. Wang, K. Q. Chen, X. F. Li, B. S. Zou and Z. Shuai, *Phys. Lett. A*, 2007, **365**, 489-494.

10 H. M. Liu, W. B. Ni, J. W. Zhao, N. Wang, Y. Guo, T. Taketsugu, M. Kiguchi and K. Murakoshi, *J. Chem. Phys.*, 2009, **130**, 244501.